DTU Library

Testing of Rotor Vortex Theories Using Betz Optimization

Okulov, Valery

Published in:
Doklady Physics

Link to article, DOI:
10.1134/S1028335814010029

Publication date:
2014

Document Version
Publisher's PDF, also known as Version of record

Citation (APA):
Okulov, V. (2014). Testing of Rotor Vortex Theories Using Betz Optimization. *Doklady Physics*, *59*(1), 16–20. https://doi.org/10.1134/S1028335814010029

ISSN 1028-3358, Doklady Physics, 2014, Vol. 59, No. 1, pp. 16–20. © Pleiades Publishing, Ltd., 2014.
Original Russian Text © V.L. Okulov, 2014, published in Doklady Akademii Nauk, 2014, Vol. 454, No. 1, pp. 37–41.

MECHANICS

Testing of Rotor Vortex Theories Using Betz Optimization

V. L. Okulov

Presented by Academician A.K. Rebrov April 25, 2013

Received June 21, 2013

DOI: 10.1134/S1028335814010029

In the beginning of the twentieth century, Ludwig Prandtl's pupil, Albert Betz, proposed a model of an optimum propeller [1]. However, first it was proved [2] that an elliptic distribution of the load along the lifting line of a finite-span wing in a uniform flow corresponds to the lowest trailing-vortex drag and provides uniform leaving of a vortex sheet from the trailing edge (Fig. 1a). Generalizing this result, Betz formulated by analogy the condition for the optimum of rotating propeller: the distribution of circulation along the lifting line replacing the blade should be such that the free vortex sheet trailing from it has an exact helical shape and moves uniformly along the axis in the direction of the main flow (Fig. 1b). If we take into account the rotation of the blade in a uniform flow giving the helical shape to the sheet leaving of the trailing edge, this model looks like an obvious consequence of the wing theory. Only in this case the circulation distribution is already asymmetrical instead of elliptic. The search for it becomes a challenge, which was not solved by Betz. In addition, a unique solution does not follow from his proof of the minimum of trailing-vortex drag for vortex sheets of an exactly helical shape because it is still necessary to set the value of a pitch of the helical sheet from additional reasons. Three proved variants are known for its determination based on different ways of taking into account the velocity induced by the vortex sheets: to neglect this velocity entirely, to take it into account from its value on the rotor, or to consider it from its double value in the far wake. In the table, we listed the well-known rotor theories with the selection of a different pitch in the vortex wake and their authors [4–8]. This paper and the analysis presented in it have the purpose to solve the problem of what pitch in the theories mentioned gives the correct result. With this purpose, the solution method [8, 9], which occurs suitable for arbitrary methods of determining the vortex-wake step, was unified for optimizing rotors with a finite number of blades. It is constructed on the use of the analytical approximation for the velocity induced by each single helical vortex filament composing a continuous wake vortex sheet [10].

The operating modes of wind turbine depend on tip speed ratio or, otherwise, the dimensionless velocity of the tip-blade rotation referred to the wind velocity; i.e.,

$$\lambda_0 = \frac{\Omega_0 R_0}{U_\infty}, \tag{1}$$

where Ω_0 is the angular velocity of the wind turbine, R_0 is its radius, and U_∞ is the unperturbed wind velocity. By analogy to the vortex theory of wings, the rotating blades are replaced by the distribution of the bounded vortices along the lifting line of the blade, while the wake is replaced by the system of free vortices in the form of fixed regular helical vortex sheets

Basic assumptions for different rotor models

Theory	Number of blades	Determination of the vortex-wake pitch
Betz–Joukowsky limit [4]	actuator disk	not determined
Glauert calculation [5] by the blade element method	not determined	both induction factors are determined in the rotor plane
Goldstein solution [6]	finite	without correction to the induction factor
Theodorsen solution [7]	finite	corrected to the induction factor in the far wake
Solution by the model [8, 9]	finite	corrected to the induction factor on the rotor

Institute of Thermophysics, Siberian Branch, Russian Academy of Sciences, Novosibirsk, 630090 Russia
Technical University of Denmark, DK-2800 Kongens Lyngby, Denmark
e-mail: vokulov@mail.ru

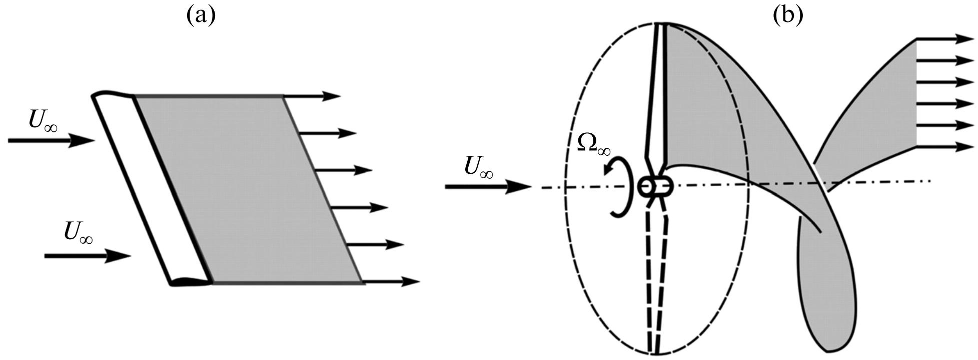

Fig. 1. (a) Prandtl vortex model of the wing with a finite span and the elliptic distribution of the load along the span [2]; (b) vortex model of the propeller proposed by Betz [1].

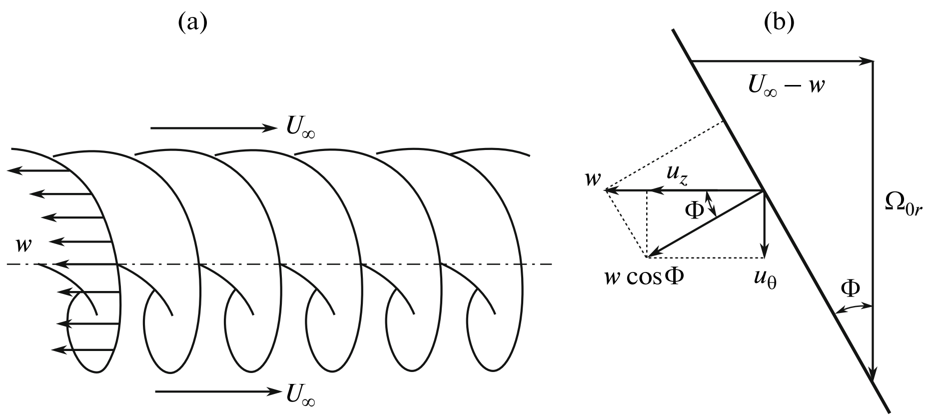

Fig. 2. (a) Schematic representation of the associated wake structure; (b) triangles of velocities: for the first wake model $w = 0$; for the second model $w = w$, and for the third model $w = \frac{1}{2}w$.

leaving from the trailing edges of blades (Fig. 1b). The load distribution along the blade in this case can be found on the basis of the Kutta–Joukowsky theorem

$$d\mathbf{L} = \rho \mathbf{U}_0 \times \mathbf{\Gamma} dr, \tag{2}$$

where $d\mathbf{L}$ is the lift acting on an element of the blade with the running size dr, $\mathbf{U}_0$ is the relative velocity of the incident flow, and Γ is the circulation of bounded vortices.

In the rotor plane, the free vortex sheet of the wake induces additional velocities u_{z_0} and u_{θ_0}; i.e., the components of relative velocity $\mathbf{U}_0$ in Eq. (2) take the form $U_{\theta_0} = \Omega r + u_{\theta_0}$ and $U_{\theta_0} = U_\infty - u_{z_0}$. For their determination, the semi-infinite system of free helical vortex sheets is replaced with the vortex system associated with it [8], which extends on both sides to infinity (Fig. 2a). According to the Helmholtz vortex theorems, the bounded circulation Γ of a blade element is unambiguously related to the circulation of the wake vortex corresponding to it in the Treftz plane, which is located far from the rotor downwards through the flow. It is clear that the velocities u_z and u_θ induced in an arbitrary cross section of the associated vortex system precisely describe the properties of the semi-infinite wake with the same distribution of circulation only in the Treftz plane. For the passage in the rotor plane, we noted that, because of symmetry, the velocity induced by a semi-infinite wake (half of the associated vortex system) is equal to half of the velocity induced at the corresponding point on the Treftz plane [1, 3]:

$$u_{\theta_0} = \frac{1}{2}u_\theta, \quad u_{z_0} = \frac{1}{2}u_z. \tag{3}$$

After integrating Eq. (2) along the lifting vortex line and summing the contribution from each blade, on the basis of Eq. (3), the power and thrust coefficients, which are made dimensionless with respect to the kinetic wind energy in the cross section equivalent to that swept by the rotor take the form

$$C_P = \frac{N_b\Omega_0}{\pi R_0^2 U_\infty^3}\int\limits_0^{R_0}\Gamma\left(U_\infty - \frac{1}{2}u_z\right)r dr,$$
$$C_T = \frac{N_b}{\pi R_0^2 U_\infty^2}\int\limits_0^{R_0}\Gamma\left(\Omega_0 r + \frac{1}{2}u_\theta\right)dr, \tag{4}$$

where N_b is the number of blades in the wind-turbine rotor. Because we neglected the wake expansion, the sheet radius coincides with the rotor radius $R \equiv R_0$. In Eq. (4), the distribution of circulation Γ along the blade and the velocities u_z and u_θ induced by the vortex sheet remain unknown. Thus, the solution is reduced to determining the radial distribution of the circulation Γ providing the equilibrium motion in the axial direction with a constant velocity wU_∞ of the associated infinite vortex sheet of the constant radius R_0 with a certain step $h = 2\pi l$ or is simply l. In the case of wind turbines, the coefficient w characterizes the deceleration of the wake motion with respect to the wind due to self-induction, i.e., the proper wake displacement under the action of velocities induced by it. The proper wake displacement can be decomposed into the normal $wU_\infty\cos\Phi$ and tangential $wU_\infty\sin\Phi$ components (Fig. 2b). Because the tangential component corresponds to the displacement of vortex particles along the sheet and does not change its position, for determining the sheet displacement, only the normal component should be taken into account. After its decomposition, the axial and circular components u_z and u_θ of the induced velocity can be written through the deceleration rate of the sheet motion in the form

$$u_\theta = wU_\infty\cos\Phi\sin\Phi, \quad u_z = wU_\infty\cos^2\Phi. \tag{5}$$

From simple geometrical reasons, these formulas can be rewritten:

$$u_\theta = wU_\infty\frac{x\bar{l}}{\bar{l}^2 + x^2}, \quad u_z = wU_\infty\frac{x^2}{\bar{l}^2 + x^2}, \tag{6}$$

where $x = \dfrac{r}{R_0}$ and $\bar{l} = \dfrac{l}{R_0}$ are the dimensionless radius and pitch.

For the vortex sheets of the still abstract arbitrarily chosen pitch l, we find the circulation Γ of their equilibrium relative motion with a constant velocity wU_∞. We introduce the dimensionless circulation in the form

$$N_b\Gamma = 2\pi l w U_\infty G(x, l). \tag{7}$$

The dimensionless radial distribution of the circulation $G(x,l)$ for an arbitrary value of the pitch in Eq. (7) is conventionally called the Goldstein function after the scientist who first solved analytically the problem of its determination but only for the cases $N_b = 2$ and 4 [4]. For its calculation at arbitrary N_b and l, we discretize each vortex layer with the help of 100 uniformly distributed single helical filament [10] between which we fulfill the condition of their motion with a constant relative velocity wU_∞. Solving the obtained set, we find the necessary distributions of circulation of this uniform motion of vortex sheets. The efficiency of the solution algorithm for this problem is confirmed in [8, 9] by good coincidence with the data calculated from the exact Goldstein solution in [11].

For obtaining the final form of power and thrust coefficients, as was already mentioned, it is necessary to set the pitch l. We consider all three variants of its determination subscripting different values with the first letter of surnames of the authors listed in the table:

(i) the step is independent of velocities induced by the wake:

$$\frac{l_B}{r} = \tan\Phi_B = \frac{U_\infty}{\Omega_0 r};$$

(ii) the step depends on the velocities induced in the far wake:

$$\frac{l_T}{r} = \tan\Phi_T = \frac{U_\infty - u_z}{\Omega_0 r + u_\theta};$$

(iii) the step depends on the velocities induced on the rotor:

$$\frac{l_O}{r} = \tan\Phi_O = \frac{U_\infty - \frac{1}{2}u_z}{\Omega_0 r + \frac{1}{2}u_\theta}.$$

The simplest first model was used in the first calculations of the rotor [1, 3, 6]. It was considered as a good approximation for weakly loaded rotors and was applied with the purpose of simplification of the solution of the problem in order that the helical pitch be independent of the induced velocities u_z and u_θ, which, in turn, themselves depend on the pitch. According to the second model introduced by Theodorsen [7], the velocities in the far wake were used for determining the pitch. At that time, it was considered that the near wake is unstable. In fact, the induced velocity should change two times in it until its final value in the far wake, where, as it seems, a steady vortex structure with a constant pitch can be formed. The third model was implemented by us in [8, 9]. After simplifying the formulas for the determination of the vortex-structure pitch in the second and third models on the basis of the formulas from the appendix in [12], we obtain for values of the pitch, respectively,

$$l_B = \frac{U_\infty}{\Omega_0} \text{ or } \frac{\Omega_0 l_B}{U_\infty} = 1; \quad l_T = \frac{U_\infty(1 - w)}{\Omega_0} \text{ or}$$

$$\frac{\Omega_0 l_T}{U_\infty} = 1 - w; \tag{8}$$

$$l_O = \frac{U_\infty\left(1 - \frac{1}{2}w\right)}{\Omega_0} \quad \text{or} \quad \frac{\Omega_0 l_O}{U_\infty} = 1 - \frac{1}{2}w.$$

Introducing the dimensionless radius $x = \frac{r}{R_0}$ and the pitch $\bar{l} = \frac{l}{R_0}$ after the substitution of Eqs. (6), (7), and (8) in Eq. (4) and identical transformations, we obtain for all cases different force coefficients:

(i) for the first rotor model according to Betz and Goldstein:

$$\begin{aligned} C_{P_B} &= w\left(2I_1(\bar{l}_B) - wI_3(\bar{l}_B)\right), \\ C_{T_B} &= w\left(2I_1(\bar{l}_B) + wI_2(\bar{l}_B)\right) \\ &\equiv w\left(I_1(\bar{l}_B)(2+w) - wI_3(\bar{l}_B)\right); \end{aligned} \tag{9}$$

(ii) for the second rotor model according to Theodorsen:

$$\begin{aligned} C_{P_T} &= w(1-w)\left(2I_1(\bar{l}_T) - wI_3(\bar{l}_T)\right), \\ C_{T_T} &= w\left(2(1-w)\, I_1(\bar{l}_T) + wI_2(\bar{l}_T)\right) \\ &\equiv w\left(I_1(\bar{l}_T)(2+w) - wI_3(\bar{l}_T)\right); \end{aligned} \tag{10}$$

(iii) for the third rotor model from [8, 9]:

$$\begin{aligned} C_{P_O} &= 2w\left(1 - \frac{1}{2}w\right)\left(I_1(\bar{l}_O) - \frac{1}{2}wI_3(\bar{l}_O)\right), \\ C_{T_O} &= 2w\left(I_1(\bar{l}_O) - \frac{1}{2}wI_3(\bar{l}_O)\right); \end{aligned} \tag{11}$$

where

$$I_1(\bar{l}) = \int_0^1 G(x,\bar{l})\,x\,dx, \quad I_2(\bar{l}) = \int_0^1 \frac{G(x,\bar{l})\,\bar{l}^2 x}{\bar{l}^2 + x^2}\,dx,$$

$$I_3(\bar{l}) = \int_0^1 \frac{G(x,\bar{l})\,x^3}{\bar{l}^2 + x^2}\,dx, \tag{12}$$

$$I_1 - I_2 = I_3.$$

When obtaining the thrust coefficient C_{T_O}, the relation $l_O\left(\Omega_0 r + \frac{1}{2}u_\theta\right) = \left(U_\infty - \frac{1}{2}u_z\right)r$ following from determining the pitch for the third model was used in (11). It is very important that force coefficients (9)–(11) for all three models at each fixed value of the vortex-sheet pitch are the functions of only one parameter—the induction factor w, which is identical for all sheet points. For this reason, it is convenient to use it for optimizing the problems. Taking into consideration that these are the power coefficient that only matter for wind turbines and that the thrust coefficient is not principal, we find at what values of w the peak efficiency is achieved. After differentiating C_P with respect to w and equating the result to zero, we find the optimum parameter specified for each pitch and model, respectively:

$$\begin{aligned} w(\bar{l}_B) &= \frac{I_1}{I_3}, \\ w(\bar{l}_T) &= \frac{2I_1 + I_3 - \sqrt{4I_1^2 - 2I_1 I_3 + I_3^2}}{3I_3}, \\ w(\bar{l}_O) &= \frac{2}{3I_3}\left(I_1 + I_3 - \sqrt{I_1^2 - I_1 I_3 + I_3^2}\right). \end{aligned} \tag{13}$$

For the limiting case, the rotor with an infinite number of blades $N_b = \infty$, the value of the Goldstein circulation has a simple form $G_\infty(x, \bar{l}) = \frac{x^2}{x^2 + \bar{l}^2}$. For it, I_1 and I_3 from Eq. (12) can be presented in a simple analytical form [9]:

$$\begin{aligned} I_1^\infty &= 1 - \bar{l}^2 \ln\frac{1+\bar{l}^2}{\bar{l}^2}, \\ I_3^\infty &= 1 + \frac{\bar{l}^2}{1+\bar{l}^2} - 2l^2 \ln\frac{1+\bar{l}^2}{\bar{l}^2}, \end{aligned} \tag{14}$$

i.e., the solutions for all optimum-rotor theories at $N_b = \infty$ are written in the analytical form through a combination of conventional functions. This limiting case is of great importance for ideal lost-free rotor models because it corresponds to the most likely value of the power coefficient for each model. Therefore, in abstract comparison of rotor theories regardless of the exact number of blades, it is expedient to analyze precisely this limiting case. According to Eq. (8), for a correct comparison of each model, it is necessary to pass from an abstract pitch to a mode parameter for controlling the wind turbine—rapidity (1) unified for all theories:

$$\lambda_0 = \frac{1}{\bar{l}_B}, \quad \lambda_0 = \frac{1 - w(\bar{l}_T)}{\bar{l}_T}, \quad \lambda_0 = \frac{1 - \frac{1}{2}w(\bar{l}_O)}{\bar{l}_O} \tag{15}$$

with the determination of w from Eq. (13). The results of the optimization for all cases are shown in Fig. 3. In the case of the operation of the rotor in the wind turbine mode, there is a restriction for the power coefficient in the form of the Betz–Joukowsky limit [4], which should not be exceeded. As a reference case, we also mention the Glauert calculation [5] obtained by the blade element momentum method section. The comparison of the power coefficients obtained for the first two wake models with them shows their inadmissibility. The first model [6] gives an absurd prediction for the possibility of 100% wind-energy utilization, and the second model [7] underestimates the limiting value. Only the third model is confirmed by the Betz–Joukowsky limit and correlates very well with the Glauert calculation. It enables us to choose this wake model from [8, 9] as the correct one completely clos-

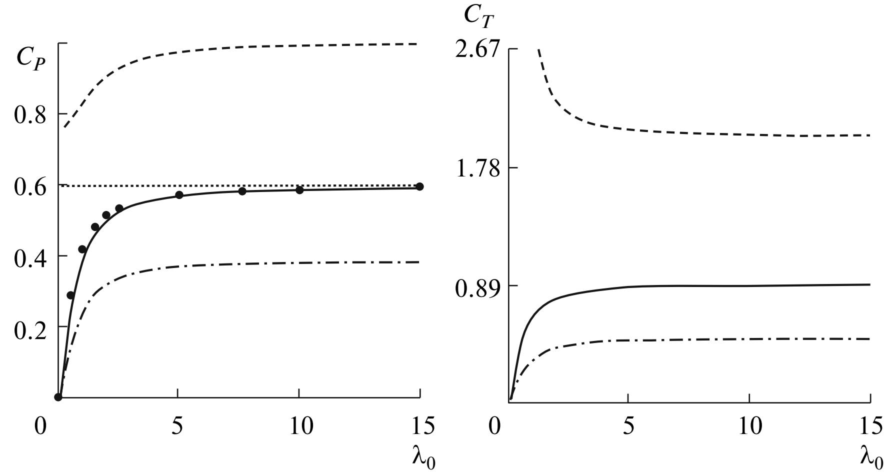

Fig. 3. The highest WEUF (C_P) and the corresponding stopping coefficient (C_T) for different rotor models: Goldstein theory (dashed line); Theodorsen theory (dash-dotted line); correct calculation by [8, 9] (solid line); Betz–Joukowski limit (dotted line); and Glauert calculation (symbols).

ing the problem. The long existence of former erroneous models [6, 7] was related to their conventional application for describing the propeller modes, where it is necessary to analyze the ratio $\frac{C_T}{C_P}$. From Fig. 3, it can be seen that, if we rule out the anomalous behavior of the thrust coefficient C_T for the first model at small λ_0, the specified ratio is approximately identical to all three wake models, which prevented for a long time establishing the mistake in the Goldstein and Theodorsen theories of rotors.

Thus, in this study, we obtained for the first time analytical solutions of the problems on the rotor optimization for three vortex models in the limiting case of an infinite number of blades. The analysis of these solutions on the rotor modes operating as the wind turbine enabled us to reveal the correct theory developed in [8, 9] and to establish the fallacy in the traditional Goldstein [6] and Theodorsen [7] optimizations. This conclusion completely agrees with the conclusions made on the basis of preliminary computations in [13].

The present work has been carried out with the support of the Danish Council for Strategic Research for the project COMWIND—Center for Computational Wind Turbine Aerodynamics and Atmospheric Turbulence (grant 2104-09-067216/DSF) (http://www.comwind.org).

REFERENCES

1. A. Betz, Schraubenpropeller mit peringstem Energieverlust: mit einem Zusatz von L. Prandtl, *Gottingen Nachrichten*, Gottingen (1919).
2. L. Prandtl, Mitteilung, Nachrichten der Gesellschaft der Wisseneschaften zu Gottingen. Math. Phys. K1, 151 (1918).
3. L. Prandtl, NACA Rept. **116**, 1 (1923).
4. V. L. Okulov and G. A. M. van Kuik, Wind Energy **15** (2), 335 (2012).
5. H. Glauert, Airplane propellers, in *Division L in Aerodynamic Theory* (Springer, Berlin, 1935), Vol. 7, pp. 169–360.
6. S. Goldstein, Proc. Roy Soc. London A **123**, 440 (1929).
7. T. Theodorsen, *Theory of Propellers* (McGraw-Hill, N.Y., 1948).
8. V. L. Okulov and J. N. Sorensen, Dokl. Phys. **53** (6), 337 (2008).
9. V. L. Okulov and J. N. Sorensen, Wind Energy **11** (4), 415 (2008).
10. V. L. Okulov, J. Fluid Mech. **521**, 319 (2004).
11. C. L. Tibery and J. W. Wrench, *Tables of Goldstein Factor*, Rept. No. 1534 (Depart. Navy, Washington, 1964).
12. V. L. Okulov and J. N. Sorensen, J. Fluid Mech. **649**, 497 (2010).
13. V. L. Okulov, J. N. Sorensen, and G. A. M. Kuik, Trudy TsAGI, No. 2713, 72 (2013).

Translated by V. Bukhanov